Vol. 25 No.2 (Juli 2024) 153-159
e-ISSN 2548-6101 p-ISSN 1411-318X

Jurnal Teknologi Lingkungan

Journal Homepage: ejournal.brin.go.id/JTL

Potential Conversion of Coconut Husk-Waste to Magnetic Cellulose Designed for Synthetic Dye Removal

Potensi Konversi Limbah Sabut Kelapa Menjadi Selulosa Magnetik untuk Penghilangan Pewarna Sintetis

ANDREAN NATAJAYA[1], FELIX NATANAEL ONGKOWIJOYO[1], MARIA YULIANA[1,2,3*], SHELLA PERMATASARI SANTOSO[1,2,3], SANDY BUDI HARTONO[1,2,3]

[1]Department of Chemical Engineering, Widya Mandala Surabaya Catholic University, Kalijudan 37, Surabaya 60114, Indonesia
[2]Chemical Engineering Master Program, Widya Mandala Surabaya Catholic University, Kalijudan 37, Surabaya 60114, Indonesia
[3]Collaborative Research Center for Zero Waste and Sustainability, Kalijudan 37, Surabaya 60114, Indonesia
*mariayuliana@ukwms.ac.id

INFORMASI ARTIKEL

Histori artikel:
Diterima 5 Februari 2024
Disetujui 2 Juli 2024
Diterbitkan 31 Juli 2024

Kata kunci:
Sabut kelapa
Selulosa
Pewarna sintetis
Adsorpsi
Degradasi

ABSTRAK

Meningkatnya kepedulian tentang keberlanjutan dan masalah lingkungan yang disebabkan oleh jumlah limbah biomassa padat yang besar di Indonesia telah mendorong upaya untuk mengembangkan produk baru untuk berbagai aplikasi di sektor energi, lingkungan, dan kesehatan. Studi ini menggunakan tempurung kelapa sebagai sumber selulosa untuk membuat selulosa magnetik (MC) melalui kopresipitasinya dengan garam besi klorida. Menggabungkan selulosa dengan nanopartikel magnetit bertujuan untuk meningkatkan laju penghilangan pewarna sintetis karena yang terakhir memberikan aktivitas katalitik yang tinggi dalam proses degradasi Fenton untuk menghilangkan polutan yang persisten. Karakteristik paramagnetik yang dimiliki oleh MC juga membuatnya mudah dipulihkan setelah digunakan. Kapasitas adsorpsi ditemukan pada 252,2 mg/g (pH 7, suhu 30°C, konsentrasi awal pewarna 100 ppm, dan rasio massa prekursor 1:4,8:25) untuk Rhodamine-B. Mineralisasi pewarna dalam kondisi ini juga mencapai 50%, menunjukkan bahwa adsorben ini dapat digunakan sebagai bahan yang efisien untuk menyerap dan mendegradasi pewarna dari larutan air. Adsorben magnetik ini akan memiliki potensi aplikasi yang besar untuk menghilangkan kontaminan organik, terutama pewarna sintetis, karena performanya yang baik, pemisahan yang sederhana, dan kemampuannya untuk melakukan proses adsorpsi dan degradasi secara bersamaan.

ARTICLE INFO

Article history:
Received 5 February 2024
Accepted 2 July 2024
Published 31 July 2024

Keywords:
Coconut husk
Cellulose
Synthetic dye
Adsorption
Degradation

ABSTRACT

Increasing concern about sustainability and environmental issues caused by the massive amount of solid biomass waste in Indonesia has driven efforts to develop new products for various endues applications in energy, environment, and health sectors. This study uses coconut husk as the cellulose source to fabricate magnetic cellulose (MC) via coprecipitation with iron chloride salts. Combining cellulose with magnetite nanoparticles aims to improve the removal rate of synthetic dye as the latter provides high catalytic activity in the Fenton degradation process to eliminate persistent pollutants. The paramagnetic characteristics that MC possesses also make them quickly recovered after use. The adsorption capacity is found at 252.2 mg/g (pH 7, temperature of 30°C, the dye initial concentration of 100 ppm, and the precursor mass ratio of 1:4.8:25) for Rhodamine-B. The dye mineralization in this condition also reaches 50%, indicating that this adsorbent can be used as an efficient material to adsorb and degrade dye from an aqueous solution. This magnetic adsorbent will be of immense potential application for removing organic contaminants, particularly synthetic dyes, due to its good performance, simple separation, and ability to perform both adsorption and degradation processes simultaneously.

1. INTRODUCTION

1.1 Background

Metal impregnation to cellulose is a promising approach to enhance the adsorption capacity of cellulose-based materials in wastewater treatment. This technique involves incorporating metal ions or nanoparticles into cellulose matrices to create composite materials with improved surface area, strength, adsorption capacity, selectivity, and chemical reactivity. The metal ions can be adsorbed onto cellulose through electrostatic interactions, allowing for the control of morphology and particle size (Mazibuko et al., 2024; Salama et al., 2021). For example, a faujasite-cellulose composite membrane has been used to remove bacteria from contaminated water, exhibiting high removal efficiency (Salama et al., 2021). However, some challenges are associated with this incorporation process; e.g., particle agglomeration and changes in the supramolecular structure of cellulose due to the incompatible nature of the component, which can deteriorate the material's mechanical properties and crystallinity index (Lesbani et al., 2015). Therefore, it is imperative to find two components with complementary properties to obtain a composite material with superior functionalities.

Water pollution is an acute environmental problem faced by many developing countries, including Indonesia. According to a report by Landrigan et al. (2018) entitled The Lancet Commission on Pollution and Health, water pollution levels increase with the development of industries in a country. Water pollution is the most significant environmental factor causing disease and premature death in the world (Landrigan et al., 2018). Various methods have been developed to address water pollution, such as precipitation and coagulation, oxidation and reduction, filtration, adsorption, photodegradation, and solid-phase extraction (Bahranowski et al., 2017; Nageeb, 2013). Of all the methods available, adsorption has been proven to be able to remove various types of pollutants by absorbing the compounds causing the pollution (adsorbate) onto the surface of the adsorbent solid (Ali et al., 2012; Keshavarzi et al., 2015). Adsorption is the most promising method, both technically and economically. Various types of adsorbents have been developed to remove toxic compounds in water.

Magnetite nanoparticles are nanomaterials that are currently being developed extensively due to their potential for application in various fields, such as water purification (Alvarez et al., 2018), biosensors (Rocha-Santos, 2014), and targeted drug delivery (Du et al., 2018). The advantages of magnetite nanoparticles include their supra-magnetic ability, high surface area and excellent porosity, good compatibility, low toxicity, and good physicochemical stability (Amiralian et al., 2020). However, there are several challenges in using magnetite nanoparticles in real-world applications. Magnetite nanoparticles can quickly oxidize and agglomerate, limiting their supra-magnetic ability and functionality (Olsson et al., 2010). On the other hand, the tiny size of magnetite nanoparticles makes them difficult to collect and remove from suspensions. Therefore, one modification that can be done to maintain the stability of magnetite dispersion is by (1) impregnating the precursor onto the polymer and (2) using the polymer as a template for the in-situ hydrolysis synthesis of magnetite nanoparticles. Several studies have been conducted to review the ability of polymer-metal composites to remove dyes (Shahriman et al., 2018; Wang et al., 2017). The research proves that polymer-metal composite materials can adsorb dyes very well. However, the fabrication of these composites is mostly done using relatively expensive synthetic polymers. Therefore, the potential utilization of cellulose derived from agricultural waste, as a medium for impregnating magnetite nanoparticles is studied.

Cellulose is known as a cheap, abundant, renewable, and biodegradable natural polymer (González et al., 2017). Cellulose fibers, which have a diameter and length in the micron range (Usmani et al., 2018), are generally composed of interconnected microfibers that form a complex network. Due to their superior mechanical properties, cellulose fibers are often used to enhance the mechanical properties of composites. Other advantages of cellulose fibers include their large surface area, low density, biodegradability, and ease of modification (Moon et al., 2011), making them a potential material for use in the production of functional biodegradable materials. The presence of hydrogen bonds between hydroxyl groups on cellulose fibers plays an important role in the composite synthesis process. They provide a network during the formation or condensation of magnetite nanoparticles (Amiralian et al., 2020), which is advantageous in increasing the impregnation rate of metal precursors on the surface of cellulose fibers. This confirms the suitability of the two single components (cellulose and magnetite) to form a composite with complementary properties.

Coconut husk waste is selected as a cellulose source due to its high cellulose content, reaching 40% of the total mass (Fatmawati et al., 2013; Kosseva, 2017). This waste is also one of the primary solid wastes in Indonesia, with a production volume of more than 7 million tons per year. The conversion of coconut husks into high-value products, such as cellulose, may reduce negative impacts on the environment. This study investigates the characteristics of magnetic cellulose (MC) composite. The performance of MC in adsorbing and degrading Rhodamine-B (RhB), one of the popular synthetic dyes, is also observed in this study to evaluate the potential utilization of coconut husk in the fabrication of MC as an adsorbent for dye removal.

1.2 Research Objectives

The objectives of this study are (1) to observe the characteristics of MC and its performance in the adsorption/degradation of RhB, and (2) to study the potential utilization of coconut husk waste in the fabrication of MC.

2. METHODS

2.1 Materials

The raw coconut husk is purchased from one of the suppliers in Bandung, Indonesia. Meanwhile, all chemicals to purify the cellulose and synthesize MC are purchased from Merck (Germany). They are of reagent grade and used as received.

2.2 Purification of Cellulose

The purification of cellulose follows the method of Fouad et al. (2020) with modifications. To extract cellulose from the fresh coconut husk, the husk was first washed, oven-dried, and ground. A 30% sodium hydroxide (w/v) solution was added to the dried coconut husk (DCH) in a ratio of 10 grams of DCH to 300 mL of NaOH solution. The mixture was stirred at 80°C for 2 h, and the treatment was repeated four times. The resulting product was then separated using filtration, washed, and filtered until it reached a neutral pH. The delignified fiber (DF) was then dried in an oven at 80°C for 12 hours.

After delignification, DF was bleached four times using a 20% hydrogen peroxide solution (solution A) with a ratio of 10 grams of DF to 150 mL of solution A. About 2% (w/v) NaOH of 2 mL was then added to the mixture and subsequently heated at 80°C for 2 h. The bleached solid (BF) was hydrolyzed using a 10% sulfuric acid solution (solution B) with a BF to solution B ratio of 10:150 (w/v, $g.ml^{-1}$). The temperature is maintained at 45°C for 1 h during the process. The resulting product was then subjected to ultrasonication, filtration, and drying to obtain purified cellulose.

2.3 Synthesis of MC

Fe_3O_4 particles were synthesized on the surface of cellulose by co-precipitation of two iron salts, namely ferric chloride hexahydrate ($FeCl_3.6H_2O$) and ferrous chloride tetrahydrate ($FeCl_2.4H_2O$) (Amiralian et al., 2020). The cellulose was initially dispersed with deionized water (0.7% (w/v)) for 30 min; then, a total of 2.2 g of $FeCl_3.6H_2O$ was added to the suspension and mixed for 1 h. The procedure is followed by the addition of 0.44 g of $FeCl_2.4H_2O$ and homogenously stirred for another hour. Subsequently, 10 mL of 25% NH_4OH solution was introduced to the mixture and agitated for 1 h until the Fe_3O_4 particles were formed and the color of the mixture turned black. The resulting solid was washed three times with ethanol and water and oven-dried for 12 h at 120°C to obtain dried magnetite-impregnated cellulose, hereinafter referred to as MC.

2.4 Characterization of MC

The crystal structure of MC is analyzed by X-ray Diffraction (XRD) analysis using the X'PERT Panalytical Pro X-ray diffractometer (Philip-FEI, Netherland) at 2θ = 5–60^0, tube current = 20 mA, running voltage = 40 kV, and constant Cu $K_{\alpha 1}$ radiation (λ = 1.5406Å). The morphology of MC is observed using a JEOL JSM-6500F (Jeol Ltd., Japan) at an accelerating voltage of 15–20 kV and a working distance of 7.5–11.0 mm. The energy-dispersive X-ray (EDX) analysis is also used to map the elements across the material surface. The adsorption/desorption profile of MC is obtained at 77 K using a Micromeritics ASAP 2010 sorption analyzer (Micromeritics Instrument Corporation, USA) after degassing the sample for 2h at 423 K. The point-of-zero-charge (pH_{pzc}) of MC is measured at a pH range of 2–12 using the drift method.

2.5 The Adsorption/Degradation Study of MC

The performance of MC in the simultaneous adsorption and degradation of RhB is studied at various initial concentrations of RhB (C_o = 25, 50, 75, 100, 125, 150, 175, 200 ppm). All adsorption experiments are conducted using a 10-mL RhB solution at neutral pH for 5 h, with an MC loading of 10 mg. The concentration of the remaining RhB in the supernatant is measured using Shimadzu UV-Vis spectrophotometer 2600 (Shimadzu, Japan) at a wavelength (λ) of 553 nm. Meanwhile, the analysis of the RhB mineralization rate is conducted using the total organic carbon (TOC) analysis performed by Mettler Toledo 6000TOCi (Mettler Toledo, USA).

The adsorption capacities (q, mg/g) and the mineralization rates (M, %) are calculated using the following equations.

$$q = \frac{(C_0 - C_f)V}{m_{MC}} \quad (1)$$

$$M\ (\%) = \frac{(TOC_0 - TOC_f)}{TOC_0} \times 100 \quad (2)$$

Where the terms of C_0 and C_f (mg/L) correspond to the initial and final RhB concentration, respectively. Meanwhile, V (L) and m_{MC} (g) are defined as the volume of RhB solution and the amount of MC. TOC_0 and TOC_f represent the initial and final TOC of RhB solution. The performance of MC for the RhB removal was then compared with that of single cellulose and magnetite.

3. RESULT AND DISCUSSION

3.1 Characterizations of MC

Cellulose with a purity of 76.51% is successfully isolated from DCH. The remaining percentage includes 5.91% of hot water soluble, 13.05% hemicellulose, 4.31% lignin, and 0.22% ash. A three-fold increase in the cellulose content from 23.55% to 76.51% can be attributed to the repeated delignification and bleaching process, which reduces the lignin content significantly. After the co-precipitation process, MC is characterized using SEM, XRD, N_2 sorption, and pH_{pzc} analysis.

The morphologies of the obtained cellulose and MC are found in Figure 1a–d. The cellulose is fiber-like and has a diameter ranging from 7–10 μm. The morphology of cellulose shows that there is an adhesion loosening between the cellulose fibrils on the cell surface (Saito et al., 2010). After the co-precipitation, the magnetite particles are seen enveloping the entire surface of cellulose, indicated by the presence of a rough surface in the matrix (Figure 1c–d). The element mapping analysis using EDX (Figure 1e) also verifies the presence of carbon, nitrogen, oxygen, and iron. The iron content in MC is observed at 31.44%, while they are 44.97% and 23.58% for carbon and oxygen, respectively. The result of the EDX characterization of the cellulose produced is that it has O and C content of 59.59% and 40.41% (w/w), respectively.

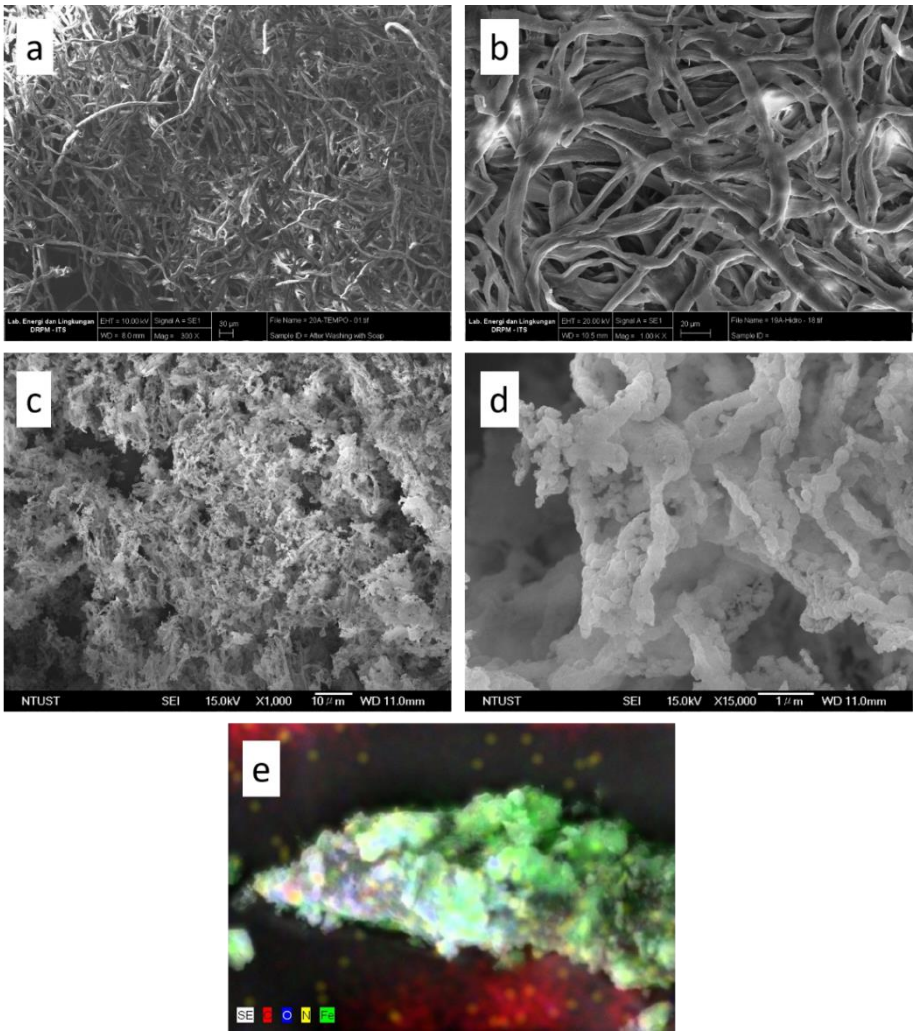

Figure 1. SEM images of (a–b) cellulose, (c–d) MC, and (e) elemental mapping of MC

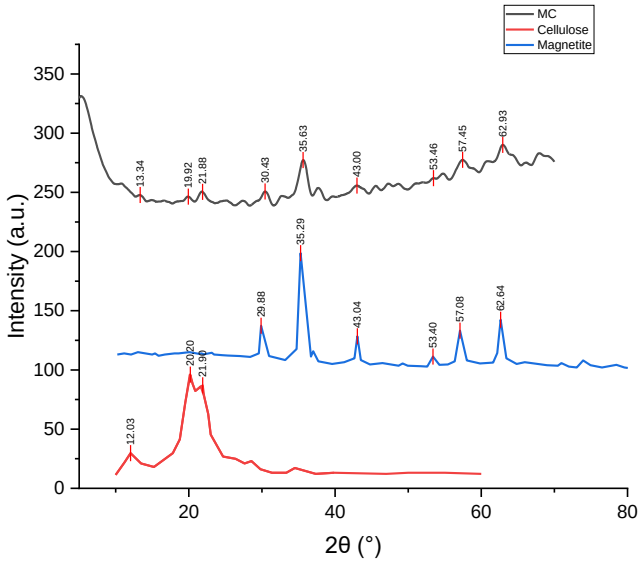

Figure 2. The diffraction spectra of MC, cellulose, and magnetite

Figure 2 shows the XRD analysis of cellulose, magnetite, and MC. Cellulose has diffraction angles at 2θ = 12.16°, 20.32°, and 21.96°, implying the presence of planar diffraction at $1\bar{1}0$, 110, and 200, in line with the characteristics of cellulose crystal II (Kolpak & Blackwell, 1976). The cellulose crystallinity is obtained at 74.5%, higher than that of reference (*ca.* 65.6%) (Rosa et al., 2010). Meanwhile, nine characteristic peaks are observed in MC, located in 2θ = 13.3°, 19.9°, 21.9°, 30.4°, 35.6°, 43.0°, 53.5°, 57.5°, and 62.9°. These peaks conform the standard pattern of cellulose and magnetite; therefore, it can be concluded that magnetite particles have been successfully deposited on the surface of cellulose.

The adsorption and desorption profile of N_2 sorption is depicted in Figure 3a. Based on the IUPAC classifications, the profile shows that MC has a mesoporous structure with the classification of IV(a). This is supported by the pore

distribution study using BJH isotherm, where MC possesses mesopores at a mean diameter = 8 nm. The observed hysteresis loop type H2(b) indicates the occurrence of narrow pore size distribution compared to the broad neck size distribution with a steep desorption curve. This type of hysteresis loop indicates the presence of pore-blocking with an ink bottle-shaped pore (Cychosz & Thommes, 2018). The surface area of MC is found at 99.839 $m^2.g^{-1}$. The pH_{pzc} determination of MC results in pH = 5.9 (Figure 3b), implying that the adsorbent has no charge at the specific pH. At pH < 5.9, the surface of MC becomes positively charged as the COO^- and OH^- ions on the surface of MC undergo protonation and bind to hydronium ions. In acidic conditions, RhB as an adsorbate also undergoes a change in charge to become cationic; therefore, MC and RhB are repulsive to each other at this pH. Moreover, the presence of H^+ ions in acidic conditions may interfere with the adsorption process, as these ions will compete with the cationic RhB to occupy the active sites of MC (Hassan et al., 2021). Conversely, when the adsorption pH is above 5.9, the surface of the adsorbent is negatively charged with COO^- and OH^- ions covering the surface, while RhB changes its form to become a zwitterion with a tendency to be positively charged. When the negatively charged MC meets RhB in the zwitterion state, an attractive force occurs between the adsorbent and the adsorbate, which may provoke the RhB adsorption (Wahyuningsih et al., 2018). Therefore, all adsorption runs are carried out at pH = 7.

3.2 Adsorption/Degradation of MC

Figure 4a shows that as the initial concentration of RhB increases, the adsorption capacity of MC will also increase until a certain point, with the highest uptake at 252.2 $mg.g^{-1}$ (pH = 7, C_o = 100 ppm, temperature = 30°C). According to Leduc et al. (2014), an increase in the concentration of the adsorbate will improve the effective collision between the adsorbate and the adsorbent and promote their interaction (Leduc et al., 2014). Moreover, a more significant concentration gradient also provides a greater driving force to reduce mass transfer resistance and ease the binding of RhB onto MC (Naidoo et al., 2019). However, a decrease in adsorption capacity occurs at C_o > 100 ppm. This is likely due to the excessively large ratio of RhB molecules to the available surface area of MC. A ratio that is too large indicates that the available adsorption sites are not proportional to the number of adsorbate particles, which causes competitive adsorption. Besides, higher concentrations of RhB can induce a more intense collision between adsorbate particles, which provoke the removal of RhB molecules from MC, leading to a lower adsorption capacity (More, 2018).

The mineralization profile of RhB indicates a declining rate at higher C_o, with the highest rate at 95.2% and C_o = 25 ppm. Similar to the discussion mentioned above, a larger ratio of RhB molecules to the binding sites of MC may reduce the chance of MC to adsorb and simultaneously degrade RhB. During the experiments, rapid mineralization of RhB to gaseous CO_2 happens almost immediately after MC is added to the RhB solution, indicated by the presence of vigorous bubbles. However, as seen from the figure, there is still some TOC remaining in the system. It implies that some dye molecules are partially degraded to the lower molecular weight components, which still contribute to the TOC content (Mahvi et al., 2009). The performance comparison of three adsorbents, single cellulose, single magnetite and MC composite are conducted, and the results are presented in Figure 4b. It can be seen that MC holds the highest uptake of RhB, as it has high textural properties and also deposited magnetite to decompose RhB.

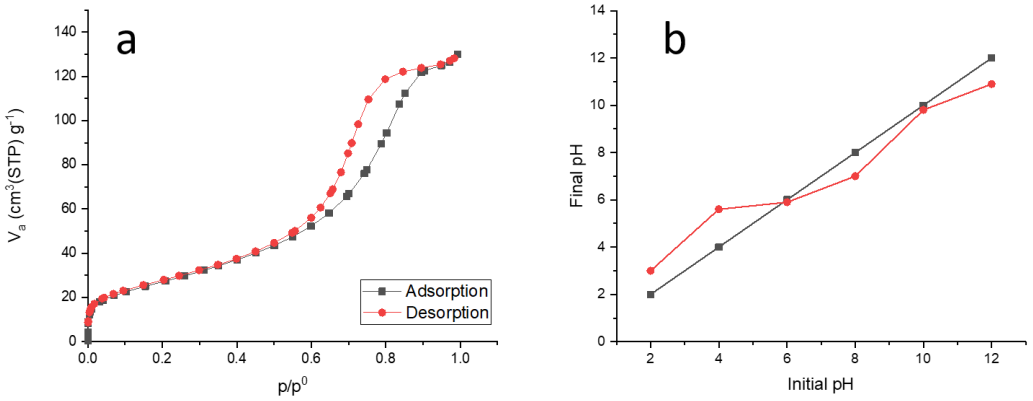

Figure 3. (a) The N_2 sorption profile and (b) pH_{pzc} of MC

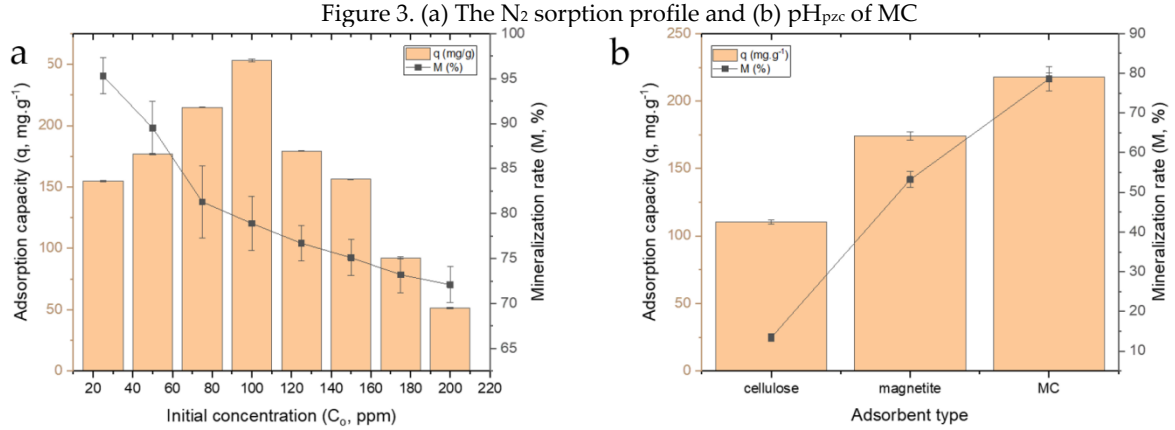

Figure 4. The adsorption capacity (q, $mg.g^{-1}$) and mineralization rate (M, %) (a) at various C_o, (b) of the three adsorbent types

4. CONCLUSION

We have successfully isolated cellulose from DCH with a purity of 76.51%, and a diameter of 7–10 μm, as well as synthesized MC via co-precipitation method. The obtained MC is characterized by rough surface of the fiber, which indicates the presence of deposited magnetite particles. The elemental mapping also confirms the presence of iron content at 31.44%. The characteristics of cellulose crystal type II is also observed at 2θ = 12.16°, 20.32°, and 21.96°. There are 9 characteristic peaks observed in the MC diffraction, which are the standard pattern of cellulose and magnetite. The surface area and average pore size of MC are found at 99.839 m2.g-1 and 8 nm, respectively. Meanwhile, the pHpzc is at pH = 5.9. In the in-situ RhB adsorption/degradation process using MC, the highest adsorption capacity (252.2 mg.g-1) is observed at pH = 7, mMC = 0.1 wt%, temperature = 30°C, Co = 100 ppm, and time = 300 min, indicating that this adsorbent can be used as an efficient material to adsorb and degrade RhB from aqueous solution. Compared with single cellulose and magnetite, MC composite has a higher removal performance of RhB, as it has the ability to perform both adsorption and degradation simultaneously. Therefore, this waste-based magnetic composite will be a promising adsorbent in the application of dye removal.

ACKNOWLEDGEMENT

The authors thank the National Taiwan University of Science and Technology (NTUST, Taiwan), and National Research and Agency, Indonesia, for providing the facilities for material characterizations. This project was supported by the Ministry of Education, Culture, Research, and Technology of the Republic of Indonesia and Widya Mandala Surabaya Catholic University through research grant no. 260C/WM01.5/N/2023, 268G/WM01.5/N/2023, and 7405/WM01/N/2022.

REFERENCES

Ali, I., Asim, M., & Khan, T. A. (2012). Low cost adsorbents for the removal of organic pollutants from wastewater. *Journal of Environmental Management*, *113*, 170–183. https://doi.org/10.1016/j.jenvman.2012.08.028

Alvarez, P. J. J., Chan, C. K., Elimelech, M., Halas, N. J., & Villagrán, D. (2018). Emerging opportunities for nanotechnology to enhance water security. *Nature Nanotechnology*, *13*(8), 634–641. https://doi.org/10.1038/s41565-018-0203-2

Amiralian, N., Mustapic, M., Hossain, M. S. A., Wang, C., Konarova, M., Tang, J., Na, J., Khan, A., & Rowan, A. (2020). Magnetic nanocellulose: A potential material for removal of dye from water. *Journal of Hazardous Materials*, *394*(February), 122571. https://doi.org/10.1016/j.jhazmat.2020.122571

Bahranowski, K., Gaweł, A., Klimek, A., Michalik-Zym, A., Napruszewska, B. D., Nattich-Rak, M., Rogowska, M., & Serwicka, E. M. (2017). Influence of purification method of Na-montmorillonite on textural properties of clay mineral composites with TiO2 nanoparticles. *Applied Clay Science*, *140*, 75–80. https://doi.org/10.1016/j.clay.2017.01.032

Cychosz, K. A., & Thommes, M. (2018). Progress in the Physisorption Characterization of Nanoporous Gas Storage Materials. In *Engineering* (Vol. 4, Issue 4, pp. 559–566). Elsevier Ltd. https://doi.org/10.1016/j.eng.2018.06.001

Du, B., Yu, M., & Zheng, J. (2018). Transport and interactions of nanoparticles in the kidneys. *Nature Reviews Materials*, *3*(10), 358–374. https://doi.org/10.1038/s41578-018-0038-3

Fatmawati, A., Agustriyanto, R., & Liasari, Y. (2013). Enzymatic hydrolysis of alkaline pretreated coconut coir. *Bulletin of Chemical Reaction Engineering and Catalysis*, *8*(1), 34–39. https://doi.org/10.9767/bcrec.8.1.4048.34-39

Fouad, H., Kian, L. K., Jawaid, M., Alotaibi, M. D., Alothman, O. Y., & Hashem, M. (2020). Characterization of microcrystalline cellulose isolated from conocarpus fiber. *Polymers*, *12*(12), 1–11. https://doi.org/10.3390/polym12122926

González, A., Contreras, C. B., Alvarez Igarzabal, C. I., & Strumia, M. C. (2017). Study of the structure/property relationship of nanomaterials for development of novel food packaging. In A. M. Grumezescu (Ed.), *Food Packaging* (pp. 265–294). Elsevier Inc. https://doi.org/10.1016/b978-0-12-804302-8.00008-x

Hassan, S. H., Velayutham, T. S., Chen, Y. W., & Lee, H. V. (2021). TEMPO-oxidized nanocellulose films derived from coconut residues: Physicochemical, mechanical and electrical properties. *International Journal of Biological Macromolecules*, *180*, 392–402. https://doi.org/10.1016/J.IJBIOMAC.2021.03.066

Keshavarzi, N., Mashayekhy Rad, F., Mace, A., Ansari, F., Akhtar, F., Nilsson, U., Berglund, L., & Bergström, L. (2015). Nanocellulose-Zeolite Composite Films for Odor Elimination. *ACS Applied Materials and Interfaces*, *7*(26), 14254–14262. https://doi.org/10.1021/acsami.5b02252

Kolpak, F. J., & Blackwell, J. (1976). Determination of the Structure of Cellulose II. *Macromolecules*, *9*(2), 273–278. https://doi.org/10.1021/ma60050a019

Kosseva, M. R. (2017). Waste From Fruit Wine Production. In P. S. Panesar & V. K. Joshi (Eds.), *Science and Technology of Fruit Wine Production* (pp. 557–598). Elsevier Inc. https://doi.org/10.1016/B978-0-12-800850-8.00011-9

Landrigan, P. J., Fuller, R., Acosta, N. J. R., Adeyi, O., Arnold, R., Basu, N. (Nil), Baldé, A. B., Bertollini, R., Bose-O'Reilly, S., Boufford, J. I., Breysse, P. N., Chiles, T., Mahidol, C., Coll-Seck, A. M., Cropper, M. L., Fobil, J., Fuster, V., Greenstone, M., Haines, A., … Zhong, M. (2018). The Lancet Commission on pollution and health. *The Lancet*, *391*(10119), 462–512. https://doi.org/10.1016/S0140-6736(17)32345-0

Leduc, J.-F., Leduc, R., & Cabana, H. (2014). Phosphate Adsorption onto Chitosan-Based Hydrogel Microspheres. *Adsorption Science & Technology*, *32*(7), 557–569.

Lesbani, A., Turnip, E. V., Mohadi, R., & Hidayati, N. (2015). Study Adsorption Desorption of Manganese(II) Using Impregnated Chitin-Cellulose as Adsorbent. *International Journal of Science and Engineering*, *8*(2), 104–108. https://doi.org/10.12777/ijse.8.2.104-108

Mahvi, A. H., Ghanbarian, M., Nasseri, S., & Khairi, A. (2009). Mineralization and discoloration of textile wastewater by TiO2 nanoparticles. *Desalination*, *239*(1–3), 309–316. https://doi.org/10.1016/j.desal.2008.04.002

Mazibuko, M. T., Onwubu, S. C., Mokhothu, T. H., Paul, V., & Mdluli, P. S. (2024). Unlocking Heavy Metal Remediation Potential: A Review of Cellulose–Silica Composites. In *Sustainability (Switzerland)* (Vol. 16, Issue 8). Multidisciplinary Digital Publishing Institute (MDPI). https://doi.org/10.3390/su16083265

Moon, R. J., Martini, A., Nairn, J., Simonsen, J., & Youngblood, J. (2011). Cellulose nanomaterials review: Structure, properties and nanocomposites. In *Chemical Society Reviews* (Vol. 40, Issue 7). https://doi.org/10.1039/c0cs00108b

More, H. (2018). *Factors Affecting Adsorption*.

Nageeb, M. (2013). Adsorption Technique for the Removal of Organic Pollutants from Water and Wastewater. *Organic Pollutants - Monitoring, Risk and Treatment*. https://doi.org/10.5772/54048

Naidoo, S., Nomadolo, N., Matshe, W. M. R., Cele, Z., & Balogun, M. (2019). Exploring the potential of N-acylated chitosan for the removal of toxic pollutants from wastewater. *IOP Conference Series: Materials Science and Engineering*, *655*(1). https://doi.org/10.1088/1757-899X/655/1/012047

Olsson, R. T., Azizi Samir, M. A. S., Salazar-Alvarez, G., Belova, L., Ström, V., Berglund, L. A., Ikkala, O., Nogués, J., & Gedde, U. W. (2010). Making flexible magnetic aerogels and stiff magnetic nanopaper using cellulose nanofibrils as templates. *Nature Nanotechnology*, *5*(8), 584–588. https://doi.org/10.1038/nnano.2010.155

Rocha-Santos, T. A. P. (2014). Sensors and biosensors based on magnetic nanoparticles. *TrAC - Trends in Analytical Chemistry*, *62*, 28–36. https://doi.org/10.1016/j.trac.2014.06.016

Rosa, M. F., Medeiros, E. S., Malmonge, J. A., Gregorski, K. S., Wood, D. F., Mattoso, L. H. C., Glenn, G., Orts, W. J., & Imam, S. H. (2010). Cellulose nanowhiskers from coconut husk fibers: Effect of preparation conditions on their thermal and morphological behavior. *Carbohydrate Polymers*, *81*(1), 83–92. https://doi.org/10.1016/j.carbpol.2010.01.059

Saito, T., Hirota, M., Tamura, N., & Isogai, A. (2010). Oxidation of bleached wood pulp by TEMPO/NaClO/NaClO2 system: Effect of the oxidation conditions on carboxylate content and degree of polymerization. *Journal of Wood Science*, *56*(3), 227–232. https://doi.org/10.1007/s10086-009-1092-7

Salama, A., Abouzeid, R., Leong, W. S., Jeevanandam, J., Samyn, P., Dufresne, A., Bechelany, M., & Barhoum, A. (2021). Nanocellulose-based materials for water treatment: Adsorption, photocatalytic degradation, disinfection, antifouling, and nanofiltration. In *Nanomaterials* (Vol. 11, Issue 11). MDPI. https://doi.org/10.3390/nano11113008

Shahriman, M. S., Mohamad Zain, N. N., Mohamad, S., Abdul Manan, N. S., Yaman, S. M., Asman, S., & Raoov, M. (2018). Polyaniline modified magnetic nanoparticles coated with dicationic ionic liquid for effective removal of rhodamine B (RB) from aqueous solution. *RSC Advances*, *8*(58), 33180–33192. https://doi.org/10.1039/C8RA06687F

Usmani, M. A., Khan, I., Gazal, U., Mohamad Haafiz, M. K., & Bhatk, A. H. (2018). Interplay of polymer bionanocomposites and significance of ionic liquids for heavy metal removal. In *Polymer-based Nanocomposites for Energy and Environmental Applications: A volume in Woodhead Publishing Series in Composites Science and Engineering*. Elsevier Ltd. https://doi.org/10.1016/B978-0-08-102262-7.00016-7

Wahyuningsih, S., Anjani, V., Munawaroh, H., & Purnawan, C. (2018). Optimization of Rhodamine B Decolorization by Adsorption and Photoelectrodegradation Combination System. *ALCHEMY Jurnal Penelitian Kimia*, *14*(2), 276. https://doi.org/10.20961/alchemy.14.2.16440.277-290

Wang, C., Wang, H., Luo, R., Liu, C., Li, J., Sun, X., Shen, J., Han, W., & Wang, L. (2017). Metal-organic framework one-dimensional fibers as efficient catalysts for activating peroxymonosulfate. *Chemical Engineering Journal*, *330*(April), 262–271. https://doi.org/10.1016/j.cej.2017.07.156